Reactions of Co-ordinated Ligands. Part 24.[1] The Reaction of Bis(but-2-yne)carbonyl(η-cyclopentadienyl or η^5-indenyl)molybdenum Tetrafluoroborate with Acetonitrile and Phosphines; Crystal Structures of But-2-ynecarbonyl(η^5-indenyl)(triethylphosphine)molybdenum Tetrafluoroborate and But-2-yne(η^5-indenyl)bis(trimethylphosphine)molybdenum Tetrafluoroborate

By **Stephen R. Allen, Paul K. Baker, Stephen G. Barnes, Michael Green,*** and **Lynda Trollope,** Department of Inorganic Chemistry, University of Bristol, Bristol BS8 1TS
Ljubica Manojlović-Muir and **Kenneth W. Muir,** Department of Chemistry, University of Glasgow, Glasgow G12 8QQ

Reaction of the compounds $[Mo(CO)(RC_2R^1)_2(\eta\text{-}C_5H_5 \text{ or } \eta^5\text{-}C_9H_7)][BF_4]$ with refluxing acetonitrile in the presence of the respective acetylene affords the compounds $[Mo(NCMe)(RC_2R^1)_2(\eta\text{-}C_5H_5 \text{ or } \eta^5\text{-}C_9H_7)][BF_4]$ where $R = R^1 = Me$; $R = Bu^t$, $R^1 = H$; $R = Ph$, $R^1 = Me$; $R = Pr^i$, $R^1 = H$. Treatment of $[Mo(CO)(RC_2R^1)_2(\eta\text{-}C_5H_5 \text{ or } \eta^5\text{-}C_9H_7)][BF_4]$ at room temperature in methylene chloride with PEt_3, PPh_3, or $P(C_6H_{11})_3$ gives the monoacetylene compounds $[Mo(CO)L(RC_2R^1)(\eta\text{-}C_5H_5 \text{ or } \eta^5\text{-}C_9H_7)][BF_4]$ [$L = PEt_3$, PPh_3, $P(C_6H_{11})_3$; $R = R^1 = Me$; $R = Bu^t$, $R^1 = H$; $R = Pr^i$, $R^1 = H$; $R = Ph$, $R^1 = Me$; or $R = R^1 = C_6H_4Me\text{-}4$]. Reaction of the acetonitrile complexes with the phosphines PEt_3, PMe_3, $PMePh_2$, $Ph_2PCH{=}CHPPh_2$, $(Ph_2PCH_2)_2$, or $(Me_2PCH_2)_2$ results in the displacement of both the acetonitrile and one acetylene ligand to form complexes of the type $[MoL_2(RC_2R^1)(\eta\text{-}C_5H_5 \text{ or } \eta^5\text{-}C_9H_7)][BF_4]$. *X*-Ray single-crystal crystallographic studies were carried out on the compounds $[Mo(CO)(PEt_3)(MeC_2Me)(\eta^5\text{-}C_9H_7)][BF_4]$ and $[Mo(PMe_3)_2(MeC_2Me)(\eta^5\text{-}C_9H_7)][BF_4]$. Crystals of the former are monoclinic, space group $P2_1/c$, $Z = 4$, in a unit cell of dimensions $a = 9.158(2)$, $b = 14.726(2)$, $c = 16.581(3)$ Å, and $\beta = 94.12(2)°$. Crystals of the latter complex are also monoclinic, space group $P2_1$, $Z = 2$, in a unit cell of dimensions $a = 8.661(2)$, $b = 10.293(2)$, $c = 13.580(2)$ Å, and $\beta = 106.42(2)°$. The structures have been refined to R 0.041 (R' 0.045) and R 0.039 (R' 0.048) for 4 329 and 2 052 respective reflections with $I > 3\sigma(I)$. The molybdenum co-ordination in each cation may be described in terms of a pseudo-octahedral structure. The but-2-yne ligand adopts a similar conformation in both complexes lying approximately coplanar with either the Mo–CO or Mo–PMe_3 bond. Variable-temperature ^1H and ^{13}C n.m.r. data are interpreted in terms of rotation of the acetylene. Examination of the ^{13}C chemical shifts of the acetylene contact carbons suggests that in these complexes the acetylene ligand can act as a four-electron donor.

THERE is currently interest in the conformational preferences and rotational barriers of carbene,[2-4] olefin,[5] and acetylene[4,6] ligands co-ordinated to η-cyclopentadienyl transition-metal species, and recently, Hoffmann and co-workers[4,7] have analysed the electronic factors controlling the rotation of the acetylene in the cations $[MoLL^1(\text{acetylene})(\eta\text{-}C_5H_5)]^+$. Previously two symmetric ($L = L^1$) complexes of this type have been synthesised, there being no examples of the asymmetric ($L \neq L^1$) case. Variable-temperature ^1H n.m.r. studies with $[Mo(dppe)(MeC_2Me)(\eta\text{-}C_5H_5)][PF_6]$ [dppe = 1,2-bis(diphenylphosphino)ethane] and $[Mo\{P(OMe)_3\}_2(MeC_2Me)(\eta\text{-}C_5H_5)][BF_4]$ suggested the most stable conformation of the acetylene to be the upright position.[6a,6b] This contrasts with the calculations for $[Mo(CO)_2(HC_2H)(\eta\text{-}C_5H_5)]^+$, which indicate a preferred conformation in which the acetylene bisects the symmetry plane of the molecule.

These complexes are also of interest in that there is the possibility[8,9] that the co-ordinated acetylene could function as a four-electron donor. Such a bonding mode is relatively uncommon for mononuclear transition-metal complexes. In this paper we describe synthetic studies affording a variety of complexes of the type $[MoLL^1(\text{acetylene})(\eta\text{-}C_5H_5)][BF_4]$, and structural studies both in the solid state and in solution leading to an understanding of the conformational preferences of these species.

RESULTS AND DISCUSSION

The starting point for this investigation was the complex $[Mo(CO)(MeC_2Me)_2(\eta\text{-}C_5H_5)][BF_4]$, which was readily available[6b] from the redox cleavage of the Mo–Mo bond present in $[\{Mo(CO)_3(\eta\text{-}C_5H_5)\}_2]$ by silver tetrafluoroborate in the presence of but-2-yne. Following our report of this synthetic approach to this and related complexes, three alternative routes to complexes of this type including those of tungsten have been reported.[10-12] Although the displacement by acetonitrile of co-ordinated carbon monoxide from metal carbonyls is a well established reaction, initial attempts to replace the carbon monoxide in the cation $[Mo(CO)(MeC_2Me)_2(\eta\text{-}C_5H_5)][BF_4]$ were unsuccessful. Thermolysis or u.v. irradiation of solutions of the cation in acetonitrile afforded deep red solutions containing free but-2-yne, and from which a crystalline product could not be obtained in satisfactory yield. However, if a solution of $[Mo(CO)(MeC_2Me)_2(\eta\text{-}C_5H_5)][BF_4]$ in acetonitrile was refluxed in the presence of an excess of but-2-yne then carbon monoxide was smoothly lost to give yellow solutions, from which the monoacetonitrile complex (3) † could be precipitated by diethyl ether in high yield. Similar reactions with $[Mo(CO)(Bu^tC_2H)_2(\eta\text{-}C_5H_5)][BF_4]$ (ref. 6*b*), (1) $[Mo(CO)$-

---

† On completion of this manuscript, Watson and Bergman reported (*J. Am. Chem. Soc.*, 1980, **102**, 2698) the preparation of the cations $[M(NCMe)(MeC_2Me)_2(\eta\text{-}C_5H_5)][PF_6]$ (M = Mo or W).

TABLE 1

Analytical [a] and infrared [b] data for the complexes $[MoL(RC_2R^1)_2(\eta\text{-}C_5H_5 \text{ or } \eta^5\text{-}C_9H_7)][BF_4]$

Complex [c]	Yield (%)	ν (cm^{-1})	Analysis (%)		
			C	H	N
(1) $[Mo(CO)(PhC_2Me)_2(\eta\text{-}C_5H_5)][BF_4]$	68	2 060, 2 040 (CO)	56.6 (56.7)	4.1 (4.1)	
(2) $[Mo(CO)(Pr^iC_2H)_2(\eta\text{-}C_5H_5)][BF_4]$	61	2 040 (CO)	46.5 (46.6)	5.2 (5.1)	
(3) $[Mo(NCMe)(MeC_2Me)_2(\eta\text{-}C_5H_5)][BF_4]$	95	2 315, 2 295 (NC)	45.0 (45.3)	5.1 (5.0)	3.4 (3.5)
(4) $[Mo(NCMe)(Bu^tC_2H)_2(\eta\text{-}C_5H_5)][BF_4]$	95	2 312, 2 293 (NC)	50.8 (50.3)	6.7 (6.2)	3.2 (3.1)
(5) $[Mo(NCMe)(PhC_2Me)_2(\eta\text{-}C_5H_5)][BF_4]$	95	2 311, 2 291 (NC)	57.2 (57.6)	4.6 (4.6)	2.7 (2.7)
(6) $[Mo(NCMe)(Pr^iC_2H)_2(\eta\text{-}C_5H_5)][BF_4]$	80	2 313, 2 295 (NC)	47.9 (47.6)	6.0 (6.5)	3.7 (3.3)
(7) $[Mo(NCMe)(MeC_2Me)_2(\eta^5\text{-}C_9H_7)][BF_4]$	95	2 320, 2 285 (NC)	50.6 (51.0)	5.1 (4.9)	3.0 (3.1)
(8) $[Mo(NCBu^t)(MeC_2Me)_2(\eta\text{-}C_5H_5)][BF_4]$	90	2 275 (NC)	49.1 (49.2)	6.0 (5.9)	3.2 (3.2)

[a] Calculated values are given in parentheses. [b] Measured in Nujol mulls. [c] All compounds are yellow.

$(PhC_2Me)_2(\eta\text{-}C_5H_5)][BF_4]$, (2) * $[Mo(CO)(Pr^iC_2H)_2(\eta\text{-}C_5H_5)][BF_4]$, and $[Mo(CO)(MeC_2Me)_2(\eta^5\text{-}C_9H_7)][BF_4]$ (ref. 6*b*) in the presence of the respective acetylene afforded the corresponding monoacetonitrile complexes (4), (5), (6), and (7) (Table 1).

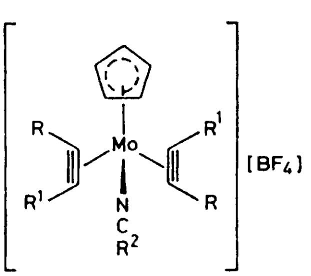

(3, R = R^1 = Me, R^2 = Me)
(4, R = H, R^1 = Bu^t, R^2 = Me)
(5, R = Me, R^1 = Ph, R^2 = Me)
(6, R = H, R^1 = Pr^i, R^2 = Me)
(8, R = R^1 = Me, R^2 = Bu^t)

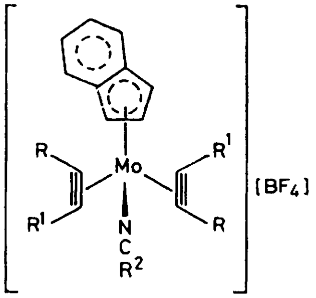

(7, R = R^1 = Me, R^2 = Me)

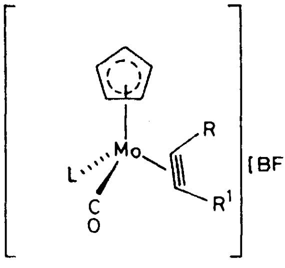

(9, L = PEt_3, R = R^1 = Me)
(10, L = PPh_3, R = R^1 = Me)
[11, L = $P(C_6H_{11})_3$, R = R^1 = Me]
(14, L = PEt_3, R = R^1 = Ph)
(15, L = PPh_3, R = R^1 = Ph)
(16, L = PPh_3, R = H, R^1 = Bu^t)
(17, L = PEt_3, R = Me, R^1 = Et)
(18, L = PPh_3, R = Me, R^1 = Et)
(19, L = PPh_3, R = Me, R^1 = Ph)
(20, L = PPh_3, R = H, R^1 = Pr^i)
(30, L = PEt_3, R = R^1 = C_6H_4Me-4)
(31, L = PPh_3, R = R^1 = C_6H_4Me-4)

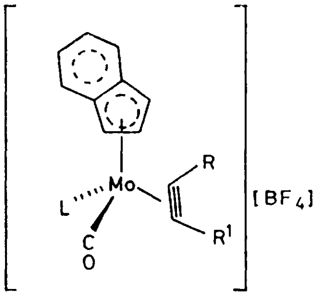

(12, L = PEt_3, R = R^1 = Me)
(13, L = PPh_3, R = R^1 = Me)

These cations are assigned the illustrated structure on the basis of elemental analyses and spectral data. The i.r. spectrum of, for example, (3) showed an asymmetric doublet at 2 315 and 2 295 cm^{-1} which is assigned to co-ordinated acetonitrile. The increase in ν(CN) on co-ordination can be ascribed to a coupling of the C–N and N–metal stretching vibrations and to an increased C–N force constant, implying [13] that the acetonitrile is functioning as a simple σ-donor ligand.

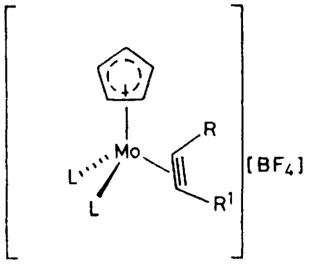

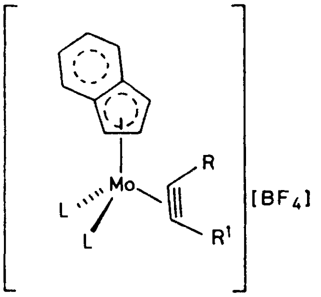

(21, L = PEt_3, R = R^1 = Me) (24, L = PMe_3, R = R^1 = Me)
(22, L = PMe_3, R = R^1 = Me)
(23, L = PMe_3, R = H, R^1 = Bu^t)
(25, L_2 = $Ph_2PCH{=\!=}CHPPh_2$, R = R^1 = Me)
(26, L_2 = $Ph_2PCH_2CH_2PPh_2$, R = R^1 = Me)
(27, L_2 = $Me_2PCH_2CH_2PMe_2$, R = R^1 = Me)
(28, L = $PMePh_2$, R = R^1 = Me)
[29, L = $P(OMe)_3$, R = R^1 = C_6H_4Me-4]

The room-temperature ^1H n.m.r. spectra (Table 2) of (3)—(7) showed the expected features for the illustrated static structures, the asymmetric acetylene complexes (4) and (5) being assigned a *transoid* configuration due to the appearance in their respective spectra of two singlets at τ 1.1 and 0.9, and τ −1.0 and 1.0 respectively, these resonances being attributable to co-ordinated acetylenic protons in different magnetic environments. The ^{13}C n.m.r. spectrum of (3) showed two acetylenic contact carbon resonances at 161.9 and 181.7 p.p.m., which can be compared with resonances at 146.2 and 165.1 p.p.m. in the corresponding spectrum of $[Mo(CO)(MeC_2Me)_2(\eta\text{-}C_5H_5)][BF_4]$. Whereas, the ^1H spectrum of $[Mo(CO)(MeC_2Me)_2(\eta\text{-}C_5H_5)][BF_4]$ is invariant up to a temperature of 363 K, above which there is evidence for loss of but-2-

---

[*] The cations (1) and (2) were prepared in high yield by an extension of the previously described [6b] synthesis of $[Mo(CO)(MeC_2Me)_2(\eta\text{-}C_5H_5)][BF_4]$.

TABLE 2

Hydrogen-1 n.m.r. data for the complexes [MoL(RC_2R^1)$_2$(η-C_5H_5 or η^5-C_9H_7)][BF_4]

Complex	L	Acetylene	^{1}H n.m.r. data (τ) *
(1)	CO	PhC_2Me	1.9—2.7 (m, 10 H, PhC$\equiv$C), 3.9—4.0 (2 s, 5 H, C_5H_5), 6.6—6.9 (3 s, 6 H, *Me*C$\equiv$C)
(2)	CO	Pr^iC_2H	−0.4, −0.3, 0.6, and 0.7(4 s, 2 H, *H*C$\equiv$C), 4.0 (s, 5 H, C_5H_5), 6.0—6.6 (m, 2 H, Me_2C*H*C$\equiv$C), 8.45—9.0 (m, 12 H, *Me*$_2$CHC$\equiv$C)
(3)	NCMe	MeC_2Me	4.2 (s, 5 H, C_5H_5), 7.0 (s, 6 H, *Me*C$\equiv$C), 7.1 (s, 3 H, *Me*CN), 7.5 (s, 6 H, *Me*C$\equiv$C). At 363 K the resonances at 7.0 and 7.5 collapsed to give one resonance at τ 7.3
(4)	NCMe	Bu^tC_2H	−1.1 (s, 1 H, *H*C$\equiv$C), 0.9 (s, 1 H, *H*C$\equiv$C), 4.2 (s, 5 H, C_5H_5), 7.1 (s, 3 H, *Me*CN), 8.6 (s, 9 H, *Bu*^{t}C$\equiv$C), 8.8 (s, 9 H, *Bu*^{t}C$\equiv$C)
(5)	NCMe	PhC_2Me	1.9—2.9 (m, 10 H, Ph), 4.1 (s, 5 H, C_5H_5), 6.6—7.6 (5 brs, 9 H, *Me*C$\equiv$C, *Me*CN)
(6)	NCMe	Pr^iC_2H	−1.0 (s, 1 H, *H*C$\equiv$C), 1.0 (s, 1 H, *H*C$\equiv$C), 4.3 (s, 5 H, C_5H_5), 6.0—6.8 (m, 2 H, Me_2C*H*C$\equiv$C), 7.1 (s, 3 H, *Me*CN), 8.4—9.1 (m, 12 H, *Me*$_2$CHC$\equiv$C)
(7)	NCMe	MeC_2Me	2.65 (m, 4 H, H^{4-7}), 3.7 [d, 2 H, $H^{2,3}$, *J*(HH) 4 Hz], 4.3 [t, 1 H, H^1, *J*(HH) 4 Hz], 7.0 (s, 3 H, *Me*CN), 7.6 (s, 6 H, *Me*C$\equiv$C), 7.8 (s, 6 H, *Me*C$\equiv$C)
(8)	$NCBu^t$	MeC_2Me	4.4 (s, 5 H, C_5H_5), 7.0 (s, 6 H, *Me*C$\equiv$C), 7.5 (s, 6 H, *Me*C$\equiv$C), 8.2 (s, 9 H, *Bu*^{t}CN)

* Measured in CD_3NO_2 at 303 K.

yne, the corresponding spectrum of the monoacetonitrile cation (3) in CD_3NO_2 is temperature dependent. The reversible spectral changes were unaffected by the addition of free but-2-yne and were consistent with methyl group site exchange ($\Delta G_{328}^{\ddagger}$ 67.5 kJ mol^{-1}) probably arising from rotation [12,14] of the but-2-yne about an axis perpendicular to the acetylenic C–C bond and passing through the molybdenum atom. This apparent lowering of the barrier to rotation on replacement of the π-acceptor carbon monoxide by the σ-donor acetonitrile is, if viewed in the context of simple σ-donor, π-acceptor electronic effects, somewhat surprising.

Whereas, trimethyl phosphite displaced both an acetylene and a carbon monoxide molecule from [Mo(CO)(MeC_2Me)$_2$(η-C_5H_5)][BF_4] (ref. 6*b*), reaction at room temperature in methylene chloride with triethylphosphine, triphenylphosphine, or tricyclohexylphosphine gave the highly coloured monocarbonyl cations (9), (10), and (11) (Table 3). The reactivity sequence $PEt_3 > PPh_3 > P(C_6H_{11})_3$ was observed, which is consistent with a steric effect paralleling the respective cone angles. A kinetic effect was also evident in the faster [with PPh_3(η-C_5H_5, 2 h), (η-C_9H_7, 0.25 h)] reaction of [Mo(CO)(MeC_2Me)$_2$(η^5-C_9H_7)][BF_4] with PEt_3 and PPh_3 giving the corresponding monocarbonyl cations (12) and (13). Thus in these reactions a phosphine selectively displaces but-2-yne. The generality of this reaction is illustrated by the ready formation of the crystalline cations (14)—(20) involving the displacement of diphenylacetylene, 3,3-dimethylbut-1-yne, pent-2-yne, 1-phenylprop-1-yne, and 3-methylbut-1-yne.

The monocarbonylphosphine cations (9)—(20) were obtained as relatively air-stable highly coloured crystalline materials, which were characterised by elemental analysis (Table 3) and i.r. and n.m.r. spectroscopy. The i.r., ^{1}H, and ^{13}C spectra exhibited (Tables 3—5) the expected general features for molecules having the molecular formula [Mo(CO)L(RC_2R^1)(η-C_5H_5 or η^5-C_9H_7)][BF_4], however, the n.m.r. spectra showed temperature-dependent behaviour consistent with the occurrence of a site-exchange process for the acetylene substituents. This is discussed later in the paper.

It is suggested that the formation of the acetonitrile and monocarbonylphosphine cations involves an initial

TABLE 3

Analytical [a] and infrared [b] data for the complexes [MoLL^1(RC_2R^1)(η-C_5H_5 or η^5-C_9H_7)][BF_4]

	Complex	Colour	Yield (%)	ν(CO) (cm^{-1})	Analysis (%)	
					C	H
(9)	[Mo(CO)(PEt_3)(MeC_2Me)(η-C_5H_5)][BF_4]	Maroon	87	1 968	42.8 (42.9)	5.9 (6.0)
(10)	[Mo(CO)(PPh_3)(MeC_2Me)(η-C_5H_5)][BF_4]	Purple	85	1 973	56.6 (56.8)	4.5 (4.4)
(11)	[Mo(CO){$P(C_6H_{11})_3$}(MeC_2Me)(η-C_5H_5)][BF_4]	Purple	67	1 959	54.7 (58.1)	7.2 (7.2)
(12)	[Mo(CO)(PEt_3)(MeC_2Me)(η^5-C_9H_7)][BF_4]	Purple	87	1 957	48.5 (48.2)	5.8 (5.6)
(13)	[Mo(CO)(PPh_3)(MeC_2Me)(η^5-C_9H_7)][BF_4]	Maroon	63	1 966	59.5 (59.8)	4.4 (4.4)
(14)	[Mo(CO)(PEt_3)(PhC_2Ph)(η-C_5H_5)][BF_4]	Purple	88	1 974	54.8 (54.6)	5.7 (5.2)
(15)	[Mo(CO)(PPh_3)(PhC_2Ph)(η-C_5H_5)][BF_4]	Blue	93	1 981	63.2 (63.7)	4.5 (4.2)
(16)	[Mo(CO)(PPh_3)(Bu^tC_2H)(η-C_5H_5)][BF_4]	Maroon	90	1 971	59.9 (58.1)	5.0 (4.8)
(17)	[Mo(CO)(PEt_3)(EtC_2Me)(η-C_5H_5)][BF_4]	Dark purple	83	1 930	43.9 (44.2)	6.0 (6.1)
(18)	[Mo(CO)(PPh_3)(EtC_2Me)(η-C_5H_5)][BF_4]	Dark purple	88	1 930	57.8 (57.4)	4.6 (4.6)
(19)	[Mo(CO)(PPh_3)(PhC_2Me)(η-C_5H_5)][BF_4]	Blue-purple	84	1 940	60.8 (60.4)	4.1 (4.3)
(20)	[Mo(CO)(PPh_3)(Pr^iC_2H)(η-C_5H_5)][BF_4]	Purple-black	80	1 990	56.5 (57.4)	4.8 (4.6)
(21)	[Mo(PEt_3)$_2$(MeC_2Me)(η-C_5H_5)][BF_4]	Royal blue	95		46.7 (46.8)	8.3 (7.6)
(22)	[Mo(PMe_3)$_2$(MeC_2Me)(η-C_5H_5)][BF_4]	Blue	74		39.2 (39.6)	6.6 (6.4)
(23)	[Mo(PMe_3)$_2$(Bu^tC_2H)(η-C_5H_5)][BF_4]	Blue	81		42.3 (42.3)	7.2 (6.8)
(24)	[Mo(PMe_3)$_2$(MeC_2Me)(η^5-C_9H_7)][BF_4]	Green-black	72		44.6 (45.2)	6.1 (6.2)
(25)	[Mo($Ph_2PCH{=}CHPPh_2$)(MeC_2Me)(η-C_5H_5)][BF_4]	Turquoise-blue	85		59.8 (60.2)	4.6 (4.7)
(26)	[Mo{$(Ph_2PCH_2)_2$}(MeC_2Me)(η-C_5H_5)][BF_4]	Green	74		60.0 (60.0)	5.0 (5.0)
(27)	[Mo{$(Me_2PCH_2)_2$}(MeC_2Me)(η-C_5H_5)][BF_4]	Turquoise	81		39.3 (39.8)	6.2 (6.0)
(28)	[Mo($PMePh_2$)$_2$(MeC_2Me)(η-C_5H_5)][BF_4]	Blue-green	82		59.2 (59.8)	5.4 (5.3)
(29)	[Mo{$P(OMe)_3$}$_2${$C_2(C_6H_4Me$-$4)_2$}(η-C_5H_5)][BF_4]	Blue	95		45.7 (46.1)	5.5 (5.3)
(30)	[Mo(CO)(PEt_3){$C_2(C_6H_4Me$-$4)_2$}(η-C_5H_5)][BF_4]	Maroon	90	1 976	56.2 (56.0)	6.0 (5.7)
(31)	[Mo(CO)(PPh_3){$C_2(C_6H_4Me$-$4)_2$}(η-C_5H_5)][BF_4]	Grey	90	1 981	64.2 (64.5)	4.7 (4.6)

[a] Calculated values are given in parentheses. [b] Measured in Nujol mulls.

TABLE 4

Hydrogen-1 n.m.r. data for the complexes $[MoLL^1(RC_2R^1)(\eta\text{-}C_5H_5 \text{ or } \eta^5\text{-}C_9H_7)][BF_4]$

Complex	L	L^1	Acetylene	^1H n.m.r. data (τ) [a]
(9) [b]	CO	PEt_3	MeC_2Me	4.06 [d, 5 H, C_5H_5, J(PH) 1 Hz], 6.62 (s, 6 H, $\mathit{Me}C{\equiv}C$); on cooling (coalescence temp. 285 K) resonances at 6.57 (s, 3 H, $\mathit{Me}C{\equiv}C$) and 6.67 (s, 3 H, $\mathit{Me}C{\equiv}C$) were observed; 9.29 (m, 6 H, $P\mathit{CH}Me$), 9.93 (m, 9 H, $PCH\mathit{Me}$)
(10) [b]	CO	PPh_3	MeC_2Me	2.61 (m, 15 H, Ph), 4.24 [d, 5 H, C_5H_5, J(PH) 2 Hz], 6.91 (s, 6 H, $\mathit{Me}C{\equiv}C$); on cooling (coalescence temp. 268 K) resonances at 6.51 (s, 3 H, $\mathit{Me}C{\equiv}C$) and 7.31 (s, 3 H, $\mathit{Me}C{\equiv}C$) were observed
(11) [b]	CO	$P(C_6H_{11})_3$	MeC_2Me	4.08 [d, 5 H, C_5H_5, J(PH) 1 Hz], 6.52 (s, 3 H, $\mathit{Me}C{\equiv}C$) and 6.70 (s, 3 H, $\mathit{Me}C{\equiv}C$); on warming (coalescence temp. 301 K) one resonance was observed at 6.61 (s, 6 H, $\mathit{Me}C{\equiv}C$); 9.02 (br m, 33 H, PC_6H_{11})
(12) [c]	CO	PEt_3	MeC_2Me	2.47—2.97 (m, 4 H, H^{4-7}), 3.74 (m, 1 H, H^3), 4.11 (m, 1 H, H^2), 4.26 [t 1 H, H^1, J(HH) 3 Hz], 6.90 (s, 3 H, $\mathit{Me}C{\equiv}C$), 8.18 (s, 3 H, $\mathit{Me}C{\equiv}C$), on warming (coalescence temp. 319 K) one resonance was observed at 7.54 (s, 6 H, $\mathit{Me}C{\equiv}C$); 8.32 (m, 6 H, $P\mathit{CH}_2Me$), 9.19 (m, 9 H, $PCH_2\mathit{Me}$)
(13) [b]	CO	PPh_3	MeC_2Me	2.54 (cm, 19 H, Ph, H^{4-7}), 3.96 (m, 2 H, H^2, H^3), 4.48 (m, 1 H, H^1), 7.76 (s, 6 H, $\mathit{Me}C{\equiv}C$); on cooling (coalescence temp. 251 K) resonances at 7.48 (s, 3 H, $\mathit{Me}C{\equiv}C$) and 7.64 (s, 3 H, $\mathit{Me}C{\equiv}C$) were observed
(14) [b]	CO	PEt_3	PhC_2Ph	2.38 (m, 10 H, Ph), 4.02 [d, 5 H, C_5H_5, J(PH) 1 Hz], 8.28 (m, 6 H, $P\mathit{CH}_2Me$), 9.02 (m, 9 H, $PCH_2\mathit{Me}$)
(15) [b]	CO	PPh_3	PhC_2Ph	2.64 (m, 25 H, Ph), 4.18 [d, 5 H, C_5H_5, J(PH) 2 Hz]
(16) [b]	CO	PPh_3	Bu^tC_2H	−2.1 (s, 1 H, $\mathit{H}C{\equiv}C$), 2.7 (m, 15 H, Ph), 4.21 [d, 5 H, C_5H_5, J(PH) 1 Hz], 8.72 (s, 9 H, Bu^t)
(17) [b]	CO	PEt_3	EtC_2Me	4.1 (s, 5 H, C_5H_5), 6.4 [q, 2 H, $CH_3\mathit{CH}_2C{\equiv}C$, ^3J(HH) 7 Hz], 6.7 (s, 3 H, $\mathit{Me}C{\equiv}C$), 8.1—8.8 (m, 9 H, $P\mathit{CH}_2Me$ and $\mathit{CH}_3CH_2C{\equiv}C$), 8.8—9.3 (m, 9 H, $PCH_2\mathit{CH}_3$)
(18) [b]	CO	PPh_3	EtC_2Me	2.3—2.8 (m, 15 H, Ph), 4.2 [d, 5 H, C_5H_5, J(PH) 1 Hz], 6.3—6.7 (m, 2 H, $CH_3\mathit{CH}_2\text{-}C{\equiv}C$), 6.9 (s, 3 H, $\mathit{Me}C{\equiv}C$), 8.7 [t, 3 H, $\mathit{CH}_3CH_2C{\equiv}C$, J(HH) 8 Hz]
(19) [b]	CO	PPh_3	PhC_2Me	2.0—2.8 (m, 20 H, PPh, $PhC{\equiv}C$), 4.1 (s, 5 H, C_5H_5), 6.8 and 7.9 (2 s, 3 H, $\mathit{Me}C{\equiv}C$)
(20) [b]	CO	PPh_3	Pr^iC_2H	2.5 (s, 1 H, $\mathit{H}C{\equiv}C$), 2.3—3.0 (m, 15 H, PPh), 4.2 [d, 5 H, C_5H_5, J(HP) 1 Hz], 6.1—6.6 (m, 1 H, $Me_2C\mathit{H}C{\equiv}C$), 8.9 and 9.05 [2 d, 6 H, Me_2CHCHC, ^3J(HH) 6 Hz]. On cooling to 183 K (coalescence temp. 223 K) resonances were observed at −2.9 and −2.7 [2 s (ratio 2 : 1), 1 H, $\mathit{H}C{\equiv}C$], 1.9—2.9 (m, 15 H, PPh), 3.85 and 3.9 [2 d, 5 H, C_5H_5, J(PH) 1 Hz], 6.1—6.6 (m, 1 H, $Me_2C\mathit{H}C{\equiv}C$), and 8.6—9.1 and 9.25 [m and d, 6 H, Me_2CH, ^3J(HH) 8 Hz]
(21) [b]	PEt_3	PEt_3	MeC_2Me	4.7 [t, 5 H, C_5H_5, J(PH) 1 Hz], 7.0 (s, 6 H, $\mathit{Me}C{\equiv}C$), 8.0—8.4 (m, 12 H, $P\mathit{CH}_2Me$), 8.8—9.2 (m, 18 H, $PCH_2\mathit{Me}$)
(22) [b]	PMe_3	PMe_3	MeC_2Me	4.6 [t, 5 H, C_5H_5, J(PH) 1.5 Hz], 7.0 (s, 6 H, $\mathit{Me}C{\equiv}C$), 8.6 [apparent d, 18 H, $P\mathit{Me}$, $\lvert {}^2J(PH) + {}^4J(PH) \rvert$ 9 Hz]
(23) [b]	PMe_3	PMe_3	Bu^tC_2H	−1.6 [t, 1 H, $\mathit{H}C{\equiv}C$, J(PH) 15 Hz], 4.5 [t, 5 H, C_5H_5, J(PH) 1 Hz], 8.5 [apparent d, 18 H, $P\mathit{Me}$, $\lvert {}^2J(PH) + {}^4J(PH) \rvert$ 9 Hz]
(24)	PMe_3	PMe_3	MeC_2Me	2.55 (m, 4 H, H^{4-7}), 4.2 [q, 2 H, H^2, H^3, J(HH) = J(HP) 2 Hz], 4.9 [t, 1 H, H^1, J(HH) 2 Hz], 7.5 (s, 6 H, $\mathit{Me}C{\equiv}C$), 8.6 [apparent d, $P\mathit{Me}$, $\lvert {}^2J(PH) + {}^4J(PH) \rvert$ 9 Hz]. At 183 K the signal at 7.5 appeared as a broad resonance. Further cooling resulted in crystallisation
(25) [c]	$L = L^1 = Ph_2PCH{=}CHPPh_2$		MeC_2Me	1.1 (m, 2 H, $PC\mathit{H}{=}CH$), 2.4—3.1 (m, 20 H, $C_6\mathit{H}_5P$), 4.76 (s, 5 H, C_5H_5), 7.16 (s, 3 H, $\mathit{Me}C{\equiv}C$), 8.54 (s, 3 H, $\mathit{Me}C{\equiv}C$). At 363 K the signals at 7.16 and 8.54 collapse to a signal at 7.86 (s, $\mathit{Me}C{\equiv}C$)
(26) [b]	$L = L^1 = (Ph_2PCH_2)_2$		MeC_2Me	2.5—3.0 (m, 20 H, $C_6\mathit{H}_5P$), 4.4 (s, 5 H, $C_5\mathit{H}_5$), 6.62 (br, 4 H, $P\mathit{CH}_2CH_2P$). At 213 K two singlets at 7.02 (3 H, $\mathit{Me}C{\equiv}C$) and 8.79 (3 H, $\mathit{Me}C{\equiv}C$) appear. At 373 K these collapse to one singlet at 7.86 (6 H, $\mathit{Me}C{\equiv}C$)
(27) [c]	$L = L^1 = (Me_2PCH_2)_2$		MeC_2Me	4.6 (s, 5 H, $C_5\mathit{H}_5$), 7.16 (s, 6 H, $\mathit{Me}C{\equiv}C$), 7.96 (br, 4 H, $P\mathit{CH}_2CH_2P$), 8.64 [d, 12 H, Me_2PCH_2, ^2J(HP) 10 Hz]
(28) [b]	$PMePh_2$	$PMePh_2$	MeC_2Me	2.5—3.3 (m, 20 H, $C_6\mathit{H}_5P$), 5.02 (s, 5 H, $C_5\mathit{H}_5$), 7.04 (s, 6 H, $MeC{\equiv}C$), 8.1 [d, 6 H, $\mathit{Me}P$, ^2J(HP) 8 Hz]
(29) [d]	$P(OMe)_3$	$P(OMe)_3$	$C_2(C_6H_4Me\text{-}4)_2$	2.61—2.70 [$(AB)_2$ pattern δ_A 2.61, δ_B 2.70, 8 H, C_6H_4, J(AB) 8 Hz], 4.1 [t, 5 H, $C_5\mathit{H}_5$, J(HP) 1 Hz], 6.4 [apparent t, 18 H, $\mathit{Me}OP$, J(HP) 11 Hz], 7.63 (s, 6 H, $\mathit{Me}C_6H_4$). On cooling to 183 K the signal at 7.63 broadens
(30) [d]	CO	PEt_3	$C_2(C_6H_4Me\text{-}4)_2$	2.26—2.53 [$(AB)_2$ pattern δ_A 2.26, δ_B 2.53, 8 H, $C_6\mathit{H}_4$, J(AB) 7 Hz], 3.77 [d, 5 H, $C_5\mathit{H}_5$, J(HP) 1 Hz], 7.54 (s, 6 H, $\mathit{Me}C_6H_4$), 8.3 (m, 6 H, $P\mathit{CH}_2CH_3$), 9.0 (m, 9 H, $PCH_2\mathit{CH}_3$). At 233 K the singlet at 7.54 collapses to two singlets of equal intensity at 7.50 and 7.56
(31) [d]	CO	PPh_3	$C_2(C_6H_4Me\text{-}4)_2$	2.6 (m, 23 H, $C_6\mathit{H}_4, \mathit{Ph}_3P$), 3.66 [d, 5 H, $C_5\mathit{H}_5$, ^3J(HP) 1 Hz], 7.54 (s, 6 H, $\mathit{Me}C_6H_4$)

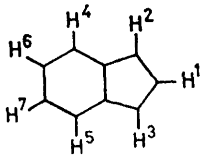

q = Quartet, cm = complex multiplet, and brd = broad doublet. [a] Measured at 303 K unless otherwise stated. [b] In CD_2Cl_2. [c] In CD_3NO_2. [d] In $(CD_3)_2CO$.

associative reaction with a donor ligand to form an 18-electron intermediate, in which the acetylene is bonded as a *two*-electron * system. Support for this suggestion derives from the observation[15] that the isostructural complexes [MCl(CF$_3$C$_2$CF$_3$)$_2$(η-C$_5$H$_5$)] (M = Mo or W) react with PPh$_3$ and CNBu^t to give the stable complexes [MoCl(PPh$_3$)(CF$_3$C$_2$CF$_3$)$_2$(η-C$_5$H$_5$)] and [WCl(CNBu^t)(CF$_3$C$_2$CF$_3$)$_2$(η-C$_5$H$_5$)]. As is illustrated in Scheme 1, the postulated 18-electron intermediate can lose either a molecule of acetylene or carbon monoxide. In the reaction with acetonitrile there is apparently a competitive reaction, which can be suppressed by the addition of free acetylene thus allowing formation of the acetonitrilebis(acetylene) cations. It is interesting that even in the presence of excess of acetylene the reaction with phosphines always leads to loss of one co-ordinated acetylene, and the formation of the monocarbonylphosphine substituted cations.

As is indicated in Scheme 1 if we assume a piano-stool (square-pyramidal geometry) configuration there are two possible isomeric forms for the 18-electron intermediate. Further work will be required in order to establish which isomer if any is preferred, and whether these are interconvertible by intra- or inter-molecular reaction paths.

Whereas, addition of trimethyl phosphite to a solution of (9) in methylene chloride led to the displacement of both CO and PEt$_3$ to form the known cation [Mo{P(OMe)$_3$}$_2$(MeC$_2$Me)(η-C$_5$H$_5$)][BF$_4$], attempts to replace the remaining carbonyl ligand in (8) with a further triethylphosphine ligand failed. Similarly, no reaction occurred on addition of excess of phosphine to the cations (9)—(20). This is explicable in terms of the known greater π-acceptor properties of P(OMe)$_3$ compared with phosphines. The discovery of a convenient route to the electron-rich cations [MoL$_2$(RC$_2$R)(η-C$_5$H$_5$ or η^5-C$_9$H$_7$)][BF$_4$] came from the observation that the acetonitrile in (3) is labile as evidenced by its exchange with NCCD$_3$ and NCBu^t, the latter reaction affording (8) [Mo(NCBu^t)(MeC$_2$Me)$_2$(η-C$_5$H$_5$)][BF$_4$]. Treatment of (3) and (7) with PEt$_3$, PMe$_3$, Ph$_2$PCH=CHPPh$_2$, Ph$_2$PCH$_2$CH$_2$PPh$_2$, Me$_2$PCH$_2$CH$_2$PMe$_2$, or PMePh$_2$ led to smooth reactions and the formation in high yield of the crystalline cations (21), (22), (24), (25), (26), (27), and (28). A similar reaction between (4) and PMe$_3$ formed the cation (23). These complexes were characterised by elemental analysis (Table 3) and n.m.r. spectroscopy (Tables 4 and 5).

TABLE 5

Carbon-13 n.m.r. data for the complexes [MoLL^1(RC$_2$R^1)(η-C$_5$H$_5$ or η^5-C$_9$H$_7$)][BF$_4$]

Complex	L	L^1	Acetylene	^{13}C n.m.r. data (p.p.m. downfield from SiMe$_4$)
(9) [a]	CO	PEt$_3$	MeC$_2$Me	229.6 [d, *C*≡C, ^2J(CP) 14 Hz], 220 (s, *C*O), 97.2 (s, C$_5$H$_5$), 21.4, 20.3 and 7.6
(10) [a]	CO	PPh$_3$	MeC$_2$Me	234 [d, *C*≡C, ^2J(CP) 12 Hz], 222 (s, *C*O), 140—130 (m, C$_6$H$_5$), 101 (s, *C*$_5$H$_5$), 23 (s, *Me*C≡C)
(13) [b]	CO	PPh$_3$	MeC$_2$Me	212.7 [d, *C*≡C, ^2J(CP) 12 Hz], 205.7 (s, *C*O), 132.8, 132.0, 130.7, 129.5, 124.9, 118.0, 117.0, 97.0, 95.4, 83.0, 19.5, 13.2
(15) [a]	CO	PPh$_3$	PhC$_2$Ph	231.6 [d, *C*≡C, ^2J(CP) 13 Hz], 200 (s, *C*O), 136, 132.9, 132.5, 132.3, 131.9, 130.3, 129.5, 98.8, 54.0
(16) [a]	CO	PPh$_3$	Bu^{t}C$_2$H	207.3 [d, *C*≡C, ^2J(CP) 12 Hz], 132.8, 132.3, 130,3 129.6, 98.2, 43.3, 31.0
(25) [b,c]	L = L^1 = Ph$_2$PCH=CHPPh$_2$		MeC$_2$Me	216 (s, *C*≡C), 201 (s, *C*≡C), 152 [(AX)$_2$ pattern, PCH=CHP, ^1J(CP) 38 Hz, ^2J(CP) 27 Hz, ^3J(CP) 11 Hz], 140—130 (m, *C*$_6$H$_5$), 99 (s, *C*$_5$H$_5$), 22 (s, *Me*C≡C), and 19 (s, *MeC*≡C)
(28) [b,d]	PMePh$_2$	PMePh$_2$	MeC$_2$Me	229 [t, *C*≡C, ^2J(CP) 11 Hz], 140—130 (m, *C*$_6$H$_5$), 98 (s, *C*$_5$H$_5$), 23 (s, *Me*C≡C), 20 [q, *Me*P, ^1J(CP) 14 Hz]

[a] In CD$_2$Cl$_2$ at 303 K. [b] In CD$_3$NO$_2$ at 303 K. [c] ^{31}P resonance (CD$_3$NO$_2$, 303 K) 97 p.p.m. (s, Ph$_2$*P*CH). [d] ^{31}P resonance (CD$_3$NO$_2$, 303 K) 2 p.p.m. (s, Ph$_2$*P*Me).

Examination of the ^{13}C n.m.r. spectra (Table 5) of these monoacetylene cations shows that the contact carbon atoms (*C*≡C) of the co-ordinated acetylene occur at low field in the range 207—230 p.p.m. If these values are compared with those reported for other acetylene complexes, for example, [Fe(CO)$_2$(MeC$_2$Me)(η-C$_5$H$_5$)][BF$_4$] [δ(^{13}C) 44 p.p.m.] (ref. 16), [Pt(MeC$_2$Me)(PPh$_3$)$_2$] (112.8 p.p.m.) (ref. 17), and [Pt(PhC$_2$Ph)(PPh$_3$)$_2$] (127.4 p.p.m.) (ref. 18), there is an indication that the bonding in the molybdenum cations is of a different type from the more usual η^2-bonding mode. A low-field H*C*≡CH ^{13}C shift has also been reported by Alt for the related complex [W(CH$_3$)(CO)(HC$_2$H)(η-C$_5$H$_5$)] (192.5, 187.4 p.p.m.) (ref. 19), and very recently[8] shifts of 206.1 and 207.1 p.p.m. have been established for the complex [W(CO)(HC$_2$H)(S$_2$CNEt$_2$)$_2$], which had previously[9] been structurally identified by *X*-ray crystallography. Both Alt's complex (τ −2.54 and −1.197) and the latter complex (τ −2.3) show extreme downfield shifts for the co-ordinated acetylene protons, and similar shifts are exhibited (Tables 2 and 4) by the cations (2), (4), (6), (16), (20), and (23). The downfield shifts for the dithiocarbamate complexes have been interpreted[20] as evidence for either a delocalised metallacyclopropenium system or more recently[9] for a bonding mode resembling a dicarbene fragment. This is, of course, an extreme valence bond description, which if extended to the molybdenum cationic complexes would imply that these complexes are co-ordinatively saturated *seven*-co-ordinate species. A more satisfactory description of these molecules is the molecular orbital (m.o.) approach adopted by Hoffmann and co-workers[4,7] where the interaction of *two* π and *two* π* acetylene levels with the respective orbitals

---

* There is evidence[8,9] for the idea that acetylenes can function in the extreme as four-electron donors. Although it is not possible in the complex [Mo(CO)(MeC$_2$Me)$_2$(η-C$_5$H$_5$)][BF$_4$] for both acetylenes to act in this way it is likely that there is a contribution from this mode of bonding, and therefore the reaction with a donor ligand (NCMe or phosphine) probably involves a switch in the bonding mode of the acetylenes to accommodate the incoming ligand.

of the fragments $[MoLL^1(\eta\text{-}C_5H_5)]^+$ ($L = L^1$ and $L \neq L^1$) are described, the conformational preferences being controlled by the splitting and reorientation of the metal donor orbitals of π symmetry.

Whatever bonding description we adopt for these molecules, an important point is the implication that acetylenes in mononuclear complexes can vary their electron-donor properties. Thus, in the reaction of complex (9) with trimethyl phosphite, which gives $[Mo\{P(OMe)_3\}_2(MeC_2Me)(\eta\text{-}C_5H_5)][BF_4]$, it is likely that the but-2-yne ligand ' switches ' its bonding mode from a four-electron donor to a two-electron donor on the approach of the $P(OMe)_3$ ligand thus allowing the formation of an 18-electron intermediate containing an η^2-bonded but-2-yne. In the case of the bis(acetylene) cations of the type $[MoL(RC_2R)_2(\eta\text{-}C_5H_5)][BF_4]$ ($L =$ CO or NCMe) it is not possible for both acetylenes to act as four-electron donors, and it is interesting that replacement of the π-acceptor CO by the σ-donor NCMe results in a downfield shift of the acetylenic contact ^{13}C resonances implying a change in bonding mode.

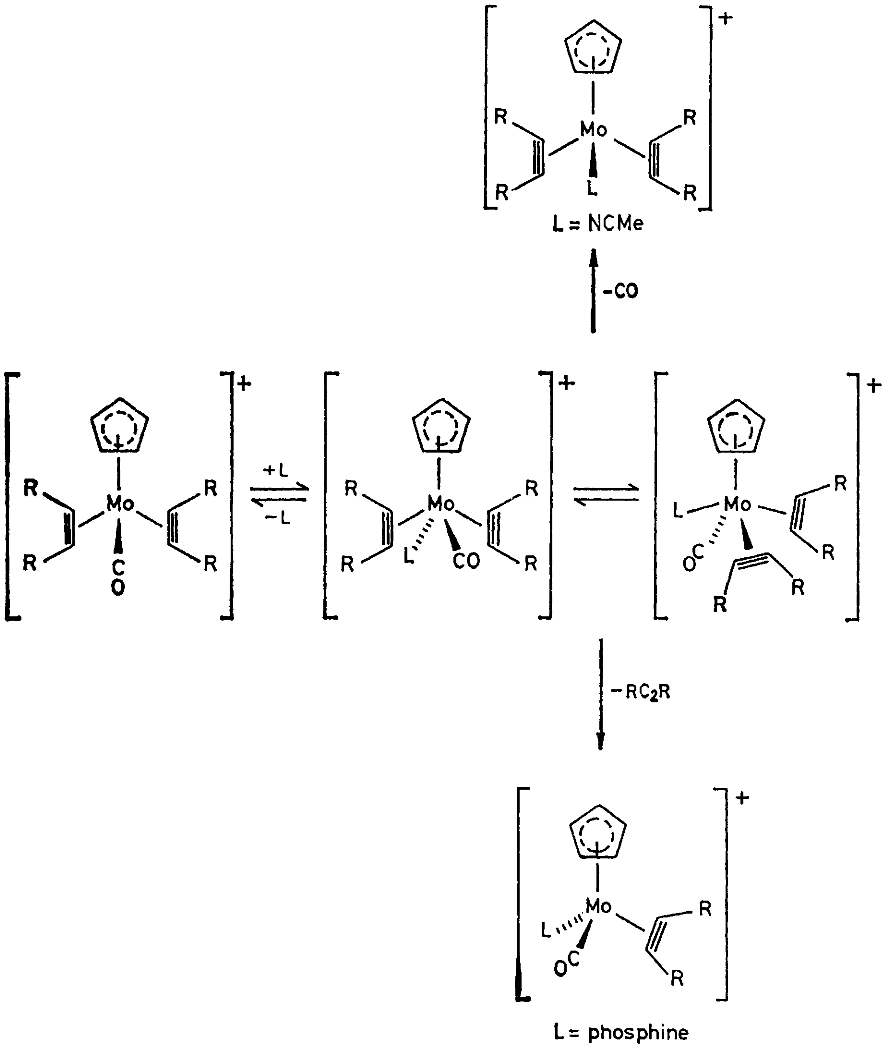

Scheme 1

The availability of complexes of the type $[MoLL^1$-(acetylene)$(\eta\text{-}C_5H_5$ or $\eta^5\text{-}C_9H_7)][BF_4]$ made it possible to examine the conformational preferences of these molecules. Single-crystal X-ray diffraction studies were therefore undertaken with a symmetrical ($L = L^1$) and an asymmetrical ($L \neq L^1$) cation.

The complexes (12) $[Mo(CO)(PEt_3)(MeC_2Me)(\eta^5\text{-}C_9H_7)]$-$[BF_4]$ and (24) $[Mo(PMe_3)_2(MeC_2Me)(\eta^5\text{-}C_9H_7)][BF_4]$ were chosen for this study, which established (see Tables 6—10) the structures shown in Figures 1 and 2. Each structure is built from well separated tetrafluoroborate anions and molybdenum centred cations, in which the molybdenum atom attains a formal 18-electron configuration by co-ordination to an η^5-C_5 indenyl ring, a but-2-yne ligand functioning as a four-electron donor, and two unidentate two-electron donor ligands [CO and PEt_3 in (12), two PMe_3 ligands in (24)]. This view of the bonding is supported by the experimentally determined ligand geometries (Tables 7 and 9) which are otherwise unexceptional. Thus the η^5-C_5 indenyl rings are approximately regular pentagons. The carbon atoms of

TABLE 6

Fractional atomic co-ordinates (× 10^4) for $[\mathrm{Mo(CO)(PEt_3)(MeC_2Me)(C_9H_7)}][\mathrm{BF_4}]$

Atom	*x*	*y*	*z*
Mo	3 833(1)	2 114(1)	686(1)
P	1 339(1)	2 451(1)	106(1)
O	3 283(4)	134(3)	144(3)
C(1)	3 458(5)	869(4)	349(3)
C(2)	4 677(5)	1 981(4)	−429(2)
C(3)	5 046(4)	2 759(3)	−118(2)
C(4)	4 803(7)	1 420(4)	−1 177(3)
C(5)	5 961(6)	3 542(4)	−278(3)
C(6)	6 809(4)	2 784(4)	1 872(3)
C(7)	7 131(5)	3 680(4)	1 820(3)
C(8)	6 019(7)	4 360(4)	1 744(3)
C(9)	4 570(6)	4 135(4)	1 707(3)
C(10)	4 186(4)	3 211(3)	1 785(2)
C(11)	5 315(4)	2 526(3)	1 868(2)
C(12)	4 613(5)	1 666(3)	1 967(2)
C(13)	3 091(5)	1 834(4)	1 988(2)
C(14)	2 819(4)	2 759(4)	1 838(2)
C(15)	828(5)	3 645(4)	69(3)
C(16)	1 878(6)	4 240(4)	−345(4)
C(17)	181(5)	2 054(4)	−940(3)
C(18)	−454(7)	2 164(5)	−1 355(4)
C(19)	−142(6)	1 954(5)	629(3)
C(20)	−289(8)	997(5)	608(4)
B	8 986(8)	305(5)	2 737(4)
F(1)	10 141(6)	798(4)	2 596(3)
F(2)	8 497(7)	462(4)	3 472(3)
F(3)	7 875(5)	406(5)	2 228(4)
F(4)	9 297(6)	−538(4)	2 773(5)

TABLE 7

Selected distances and angles in $[\mathrm{Mo(CO)(PEt_3)(MeC_2Me)(C_9H_7)}][\mathrm{BF_4}]$

(*a*) Bond lengths (Å)

Mo–P	2.464(1)	C(2)–C(3)	1.291(7)
Mo–C(1)	1.941(5)	C(2)–C(4)	1.502(6)
Mo–C(2)	2.063(4)	C(3)–C(5)	1.462(7)
Mo–C(3)	2.030(4)	C(6)–C(7)	1.357(7)
Mo–C(10)	2.439(4)	C(6)–C(11)	1.419(6)
Mo–C(11)	2.381(4)	C(7)–C(8)	1.426(8)
Mo–C(12)	2.289(4)	C(8)–C(9)	1.365(7)
Mo–C(13)	2.347(4)	C(9)–C(10)	1.414(7)
Mo–C(14)	2.381(4)	C(10)–C(11)	1.445(6)
P–C(15)	1.820(5)	C(10)–C(14)	1.426(6)
P–C(17)	1.829(4)	C(11)–C(12)	1.435(6)
P–C(19)	1.816(5)	C(12)–C(13)	1.418(6)
F(1)–B	1.318(7)	C(13)–C(14)	1.404(7)
F(2)–B	1.349(8)	C(15)–C(16)	1.502(8)
F(3)–B	1.282(8)	C(17)–C(18)	1.529(7)
F(4)–B	1.274(8)	C(19)–C(20)	1.416(10)
O–C(1)	1.142(6)		

(*b*) Bond angles (°)

P–Mo–C(1)	86.4(1)	C(7)–C(8)–C(9)	121.3(5)
P–Mo–C(2)	93.8(1)	C(8)–C(9)–C(10)	118.5(5)
P–Mo–C(3)	100.7(1)	C(9)–C(10)–C(11)	120.0(4)
C(1)–Mo–C(2)	73.9(2)	C(9)–C(10)–C(14)	132.9(4)
C(1)–Mo–C(3)	110.3(2)	C(11)–C(10)–C(14)	107.1(4)
Mo–P–C(15)	115.9(2)	C(6)–C(11)–C(10)	119.8(4)
Mo–P–C(17)	111.0(2)	C(6)–C(11)–C(12)	132.5(4)
Mo–P–C(19)	115.9(2)	C(10)–C(11)–C(12)	107.6(4)
C(15)–P–C(17)	105.2(2)	C(11)–C(12)–C(13)	107.4(4)
C(15)–P–C(19)	101.9(3)	C(12)–C(13)–C(14)	109.1(4)
C(17)–P–C(19)	105.9(3)	C(10)–C(14)–C(13)	108.5(4)
Mo–C(1)–O	177.8(5)	P–C(15)–C(16)	114.1(4)
Mo–C(2)–C(3)	70.2(3)	P–C(17)–C(18)	116.4(4)
Mo–C(2)–C(4)	148.1(4)	P–C(19)–C(20)	117.5(5)
C(3)–C(2)–C(4)	141.7(5)	F(1)–B–F(2)	112.8(6)
Mo–C(3)–C(2)	73.0(3)	F(1)–B–F(3)	115.4(7)
Mo–C(3)–C(5)	146.8(4)	F(1)–B–F(4)	111.5(7)
C(2)–C(3)–C(5)	139.8(4)	F(2)–B–F(3)	106.0(7)
C(7)–C(6)–C(11)	118.3(5)	F(2)–B–F(4)	102.2(7)
C(6)–C(7)–C(8)	122.1(5)	F(3)–B–F(4)	108.0(8)

TABLE 8

Fractional atomic co-ordinates (× 10^n, $n = 5$ for Mo, 4 otherwise) for $[\mathrm{Mo(PMe_3)_2(MeC_2Me)(C_9H_7)}][\mathrm{BF_4}]$

Atom	*x*	*y*	*z*
Mo	3 386(6)	25 000	22 795(4)
P(1)	2 170(3)	999(3)	3 396(2)
P(2)	1 790(3)	4 470(3)	2 998(2)
C(1)	657(10)	2 866(8)	905(6)
C(2)	1 898(9)	2 194(8)	1 438(6)
C(3)	16(15)	3 409(14)	−155(7)
C(4)	3 437(12)	1 717(14)	1 229(11)
C(5)	−3 000(13)	1 261(12)	750(10)
C(6)	−3 711(14)	1 998(14)	−113(11)
C(7)	−3 850(15)	3 349(11)	7(10)
C(8)	−3 152(15)	3 986(12)	893(10)
C(9)	−2 439(13)	3 249(10)	1 777(10)
C(10)	−2 365(13)	1 878(10)	1 711(10)
C(11)	−1 602(15)	1 361(11)	2 689(10)
C(12)	−1 300(9)	2 497(16)	3 395(6)
C(13)	−1 738(14)	3 591(11)	2 847(9)
C(14)	1 725(19)	554(14)	4 603(8)
C(15)	4 332(13)	1 325(14)	3 910(12)
C(16)	2 114(15)	−614(10)	2 783(11)
C(17)	3 910(16)	4 553(15)	3 016(15)
C(18)	983(21)	5 893(10)	2 230(12)
C(19)	1 896(19)	4 955(15)	4 312(10)
B	2 916(20)	2 770(15)	7 092(14)
F(1)	3 238(17)	1 568(10)	7 336(11)
F(2)	4 022(15)	2 947(25)	6 619(18)
F(3)	1 528(11)	3 053(9)	6 442(7)
F(4)	3 125(30)	3 487(15)	7 837(11)

TABLE 9

Selected distances and angles in $[\mathrm{Mo(PMe_3)_2(MeC_2Me)(C_9H_7)}][\mathrm{BF_4}]$

(*a*) Bond lengths (Å)

Mo–P(1)	2.417(3)	C(1)–C(3)	1.497(13)
Mo–P(2)	2.439(3)	C(2)–C(4)	1.521(14)
Mo–C(1)	1.999(8)	C(5)–C(6)	1.386(19)
Mo–C(2)	2.025(8)	C(5)–C(10)	1.415(18)
Mo–C(9)	2.433(11)	C(6)–C(7)	1.409(19)
Mo–C(10)	2.339(11)	C(7)–C(8)	1.353(18)
Mo–C(11)	2.245(12)	C(8)–C(9)	1.407(17)
Mo–C(12)	2.350(7)	C(9)–C(10)	1.417(15)
Mo–C(13)	2.423(11)	C(9)–C(13)	1.450(17)
P(1)–C(14)	1.846(12)	C(10)–C(11)	1.410(17)
P(1)–C(15)	1.835(11)	C(11)–C(12)	1.487(18)
P(1)–C(16)	1.851(12)	C(12)–C(13)	1.344(19)
P(2)–C(17)	1.831(13)	B–F(1)	1.291(18)
P(2)–C(18)	1.819(13)	B–F(2)	1.31(2)
P(2)–C(19)	1.829(13)	B–F(3)	1.309(19)
C(1)–C(2)	1.311(11)	B–F(4)	1.22(2)

(*b*) Bond angles (°)

P(1)–Mo–P(2)	96.2(1)	Mo–C(2)–C(4)	156.2(7)
P(1)–Mo–C(1)	117.8(2)	C(1)–C(2)–C(4)	133.8(9)
P(1)–Mo–C(2)	80.2(2)	C(6)–C(5)–C(10)	119.9(12)
P(2)–Mo–C(1)	91.4(2)	C(5)–C(6)–C(7)	118.3(12)
P(2)–Mo–C(2)	90.2(2)	C(6)–C(7)–C(8)	123.4(12)
Mo–P(1)–C(14)	116.8(5)	C(7)–C(8)–C(9)	118.4(11)
Mo–P(1)–C(15)	122.7(5)	C(8)–C(9)–C(10)	120.0(11)
Mo–P(1)–C(16)	111.3(4)	C(8)–C(9)–C(13)	133.0(10)
Mo–P(2)–C(17)	116.5(5)	C(10)–C(9)–C(13)	107.0(10)
Mo–P(2)–C(18)	111.6(5)	C(9)–C(10)–C(5)	119.5(11)
Mo–P(2)–C(19)	119.6(5)	C(9)–C(10)–C(11)	109.5(10)
C(14)–P(1)–C(15)	98.9(7)	C(5)–C(10)–C(11)	131.0(11)
C(14)–P(1)–C(16)	101.0(6)	C(10)–C(11)–C(12)	105.1(10)
C(15)–P(1)–C(16)	103.2(6)	C(11)–C(12)–C(13)	109.4(8)
C(17)–P(2)–C(18)	101.0(7)	C(9)–C(13)–C(12)	108.9(10)
C(17)–P(2)–C(19)	101.6(8)	F(1)–B–F(2)	97(2)
C(18)–P(2)–C(19)	104.2(7)	F(1)–B–F(3)	119(2)
Mo–C(1)–C(2)	72.1(5)	F(1)–B–F(4)	113(2)
Mo–C(1)–C(3)	149.0(7)	F(2)–B–F(3)	107(2)
C(2)–C(1)–C(3)	138.7(9)	F(2)–B–F(4)	111(2)
Mo–C(2)–C(1)	69.9(5)	F(3)–B–F(4)	108(2)

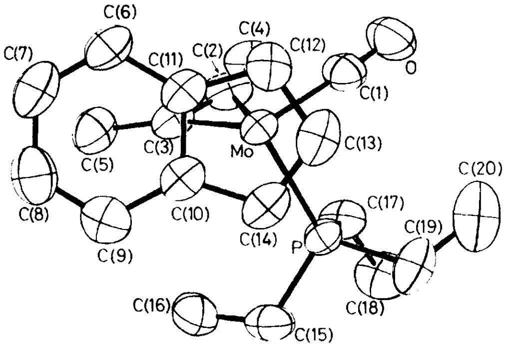

FIGURE 1 The $[Mo(CO)(PEt_3)(MeC_2Me)(C_9H_7)]^+$ cation viewed normal to the indenyl ligand. Here, and in Figure 2, 50% probability ellipsoids are shown

each but-2-yne ligand lie within ±0.02 Å of their common plane, which passes close to the associated molybdenum atom [displacements 0.064 Å in (12) and 0.026 Å in (24)].

TABLE 10

Comparison of bond angles (°) subtended at the molybdenum atom in (12) and (24). A is the midpoint of the η^2-C≡C bond and B is the terminus of the Mo→η^5-C_5(ring) normal

(12)		(24)	
A–Mo–B	141	A–Mo–B	139
A–Mo–P	98	A–Mo–P(1)	99
A–Mo–C(1)	92	A–Mo–P(2)	91
B–Mo–P	112	B–Mo–P(1)	109
B–Mo–C(1)	115	B–Mo–P(2)	114
P–Mo–C(1)	86	P(1)–Mo–P(2)	96

The presence of the strongly π-acidic carbonyl ligand in (12) is the most likely explanation for the slight (0.01—0.03 Å) lengthening, compared with (24), of corresponding Mo–ligand distances. Thus the Mo–P bond lengths are 2.464(1) Å in (12) and 2.417(3) and 2.439(3) Å in (24). In both cations the Mo–C(but-2-yne) distances are slightly irregular [2.063(4) and 2.030(4) Å in (12) and 2.025(8) and 1.999(8) Å in (24)]. No other Mo–C(alkyne) bond lengths are available with which to make comparisons, and even if such data were available it would be difficult to differentiate between the various factors influencing the bond lengths. However, these bond lengths are certainly shorter than might have been expected. This possibly relates to an important contribution from the four-electron bonding mode.

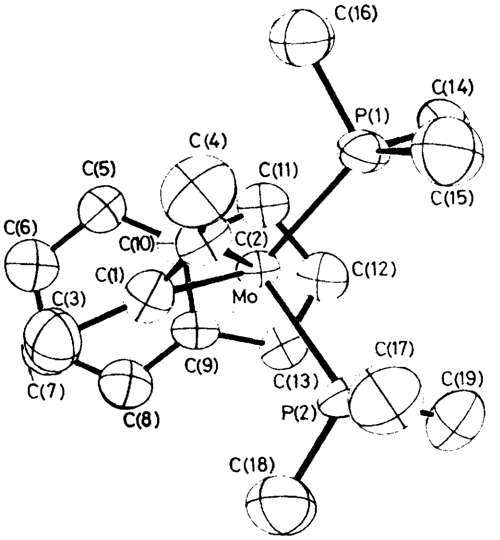

FIGURE 2 The $[Mo(PMe_3)_2(MeC_2Me)(C_9H_7)]^+$ cation viewed normal to the indenyl ligand

In both (12) and (24) the Mo–C(indenyl) bond lengths are also rather irregular [2.29—2.44 Å in (12), 2.25—2.43 Å in (24)] but the displacement of the molybdenum atom from the η^5-C_5 plane in (12) [2.030(1) Å] is again slightly greater than the corresponding value [2.016(1) Å] in (24).

The molybdenum co-ordination in (12) and (24) may conveniently be regarded as pseudo-octahedral. Three facial sites are occupied by two unidentate ligands and by A, the midpoint of the but-2-yne C≡C bond. The remaining three are occupied by the η^5-C_5 indenyl ring. In each cation the acetylene adopts a similar position under the indenyl ligand and the metal co-ordination is distorted so as to increase the angle between these ligands. Thus, if B is the terminus of the Mo–η^5-C_5 ring normal, the A–Mo–B angles are 141° and 139° in (12) and (24) respectively [*cf.* B–Mo–P 112°, B–Mo–C(1) 115° in (12), B–Mo–P(1) 109°, B–Mo–P(2) 114° in (24)]. These angles would be 125.3° if the metal co-ordination were exactly octahedral with the Mo–B vector symmetrically positioned relative to the octahedral axes. The similarity of the molybdenum environments in (12) and (24) is particularly striking when the corresponding valency angles are compared (Table 10). The most obvious difference is the acuteness of the P–Mo–C(1) angle of 86° in (12) compared with the P(1)–Mo–P(2) angle of 96° in (24), which is easily understood in terms of the differing steric demands of carbonyl compared with trimethylphosphine.

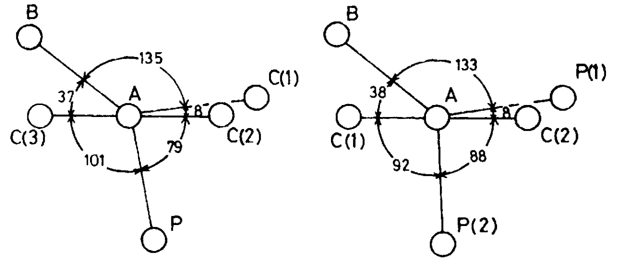

(12) (24)

FIGURE 3 The disposition of the but-2-yne ligand with respect to the metal co-ordination polyhedron in (12) and (24). In each case the view is along the A–Mo vector (see caption to Table 10). Angles (°) are X–A–Mo–Y torsion angles. To emphasise its similarity to (24) the drawing of (12) corresponds to a cation related by the operation ($\bar{x}$, $\bar{y}$, $\bar{z}$) to that described by Table 6 and Figure 1

The resemblances between the complex cations in (12) and (24) extend to the orientation (conformation) of the but-2-yne ligands, as may be seen from Figure 3, in which the torsion angles about the A–Mo bonds are compared. In (12) the C≡C bond is nearly parallel to the Mo–C(carbonyl) bond while in (24) it is almost eclipsed by the Mo–P(1) bond. This conformation appears to explain the previously noted differences in the Mo–C-(but-2-yne) distances in each complex, the nearly eclipsed carbon atom [C(2) in both (12) and (24)] being slightly further from the metal atom in each case.

The but-2-yne conformation in (12) allows favourable overlap between a filled metal *d* orbital and a vacant π^* orbital, and it is predicted by Hoffmann and coworkers [4,7] to be the minimum-energy conformation for such an asymmetric ($L = CO$, $L^1 = PEt_3$) system. For the symmetric ($L = L^1 = PMe_3$) complex (24) the theoretical situation is less clear. Hoffmann's semi-empirical m.o. calculations suggest that, for the cation $[Mo(CO)_2(HC_2H)(\eta\text{-}C_5H_5)]^+$, the stable conformation should be a symmetrical bisecting one, with B–Mo–A–C-(alkyne) torsion angles of 90°. Replacement of two carbonyl ligands by the phosphine ligands, to give a species more comparable with (24), would in our estimation be more likely to alter the height of the energy barriers to rotation rather than the position of the minimum. Thus, the but-2-yne conformation in (24), unlike that in (12), appears to be in conflict with current theoretical predictions. At present we can only note this conflict and at the same time express our view that the conformational resemblances between (12) and (24) are strong enough to suggest that broadly similar factors must determine the but-2-yne conformation observed in each complex.

TABLE 11

Activation energies for acetylene site exchange in $[MoLL^1(acetylene)(\eta\text{-}C_5H_5 \text{ or } \eta^5\text{-}C_9H_7)][BF_4]$

Complex	L	L^1	Acetylene	T_c(K) [a]	$\Delta\gamma$(Hz) [b]	$\Delta G^\ddagger_{T_c}$ (kJ mol^{-1}) [c]
(9)	CO	PEt_3	MeC_2Me	285	9	62.6
(10)	CO	PPh_3	MeC_2Me	268	81	53.8
(11)	CO	$P(C_6H_{11})_3$	MeC_2Me	301	18	64.5
(12)	CO	PEt_3	MeC_2Me	319	127	62.3
(13)	CO	PPh_3	MeC_2Me	251	15	53.6
(21)	PEt_3	PEt_3	MeC_2Me	<183		
(22)	PMe_3	PMe_3	MeC_2Me	<183		
(25)	$L = L^1 = Ph_2PCH{=}CHPPh_2$		MeC_2Me	333	143	66.0
(26)	$L = L^1 = (Ph_2PCH_2)_2$		MeC_2Me	306	177	60.0
(27)	$L = L^1 = (Me_2PCH_2)_2$		MeC_2Me	220	8	47.0
(28)	$PMePh_2$	$PMePh_2$	MeC_2Me	190	78	38.0
(29)	$P(OMe)_3$	$P(OMe)_3$	$C_2(C_6H_4Me\text{-}4)_2$	<183		
(30)	CO	PEt_3	$C_2(C_6H_4Me\text{-}4)_2$	253	6	56.0

[a] Maximum error in measuring the temperature is ±5 K. [b] Maximum error in measuring $\Delta\gamma$ is ±2 Hz. [c] Maximum estimated error ±2 kJ mol^{-1}.

With the establishment of the solid-state structure of (12) and (24) their behaviour and that of their related complexes in solution were examined. Variable-temperature ^1H n.m.r. studies on the complexes (9)—(13), (21), (22), and (24)—(28) showed that the but-2-yne is fluxional at ambient temperatures and above. On cooling, coalescence occurred leading eventually to the appearance in the ^1H spectra of two distinct *Me*C≡C resonances. The activation barriers, $\Delta G^\ddagger$, for these exchange processes were calculated from the Gutowsky–Holm [21,22] equations and are listed along with the observed coalescence temperatures in Table 11. The intramolecular nature of the exchange process was confirmed by examination of the ambient-temperature ^{13}C n.m.r. spectra (Table 5), which showed ^{31}P coupling to the acetylenic contact carbons. In order to examine the possible steric effects of the acetylene the di-4-tolylacetylene complexes (29)—(31) were synthesised and characterised (Tables 2, 3, and 5). The activation energies for methyl group (4-*Me*C_6H_4C≡C) site exchange are listed for comparison in Table 11.

Whilst the low-temperature limiting ^1H spectra of the monocarbonyl phosphine cations are consistent with a conformation in solution the same as that established in the solid state for (12), they do not establish a unique conformation, because of the asymmetry of the complexes. Similarly, the ambient-temperature ^1H spectrum of the asymmetric 3-methylbut-1-yne complex (20), which shows a single resonance at τ —2.5 but on cooling to 223 K gives resonances at τ —2.9 and —2.7 in the ratio of 2 : 1, suggests that in the slow exchange limit the two conformations (I) and (II) are not equally populated.

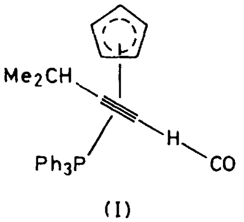

(I)

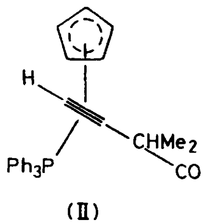

(II)

The low-temperature limiting spectrum of (26) was identical to that reported [6a] for the corresponding hexafluorophosphate salt, and along with the symmetrical complexes (25), (27), and (28) showed *two Me*C≡C ^1H resonances at low temperature. This suggests that in solution the lowest-energy conformation is similar to that established in the solid state for (24), that is where the acetylene points along the Mo–P axis. As discussed earlier this is at variance with theory. Attempts to freeze out the rotation of (21), (22), and (29) were unsuccessful.

Thus, the energy profiles for the rotation of an acetylene about the metal–acetylene bond in the d^4 systems

$[Mo(CO)(PR_3)(MeC_2Me)(\eta\text{-}C_5H_5)]^+$ and $[Mo(PR_3)_2(MeC_2Me)(\eta\text{-}C_5H_5)]^+$ are probably as shown in Scheme 2. In agreement with the theory, the size of the barriers to rotation is governed by the reduction of the symmetry. Calculated[4,7] values for $\Delta G^{\ddagger}$ with $[Mo(CO)_2(HC_2H)(\eta\text{-}C_5H_5)]^+$ (53 kJ mol^{-1}) and $[Mo(CO)(PH_3)(HC_2H)(\eta\text{-}C_5H_5)]^+$ (71 kJ mol^{-1}) are in general agreement with the experimental values listed in Table 11.

Although it is difficult to distinguish between steric and electronic influences on the magnitude of the $\Delta G^{\ddagger}$ values, examination of the data for complexes (9)—(13) in Table 11 suggests a dominant electronic effect. Thus, $P(C_6H_{11})_3$ and PEt_3, which have very different cone angles but similar σ-donor and π-acceptor properties, have almost identical barriers, whereas, PPh_3, with an intermediate steric requirement and a degree of π-acid character, has a markedly lower site-exchange barrier. The absence of a marked steric effect is again emphasised if the pairs of cyclopentadienyl and indenyl complexes (9) and (12), and (10) and (13) are compared. The difference in $\Delta G^{\ddagger}$ values observed for the cations (9) and (30) again implies the absence of a steric effect, however, it is possible that this difference arises due to steric destabilisation of the ground state.

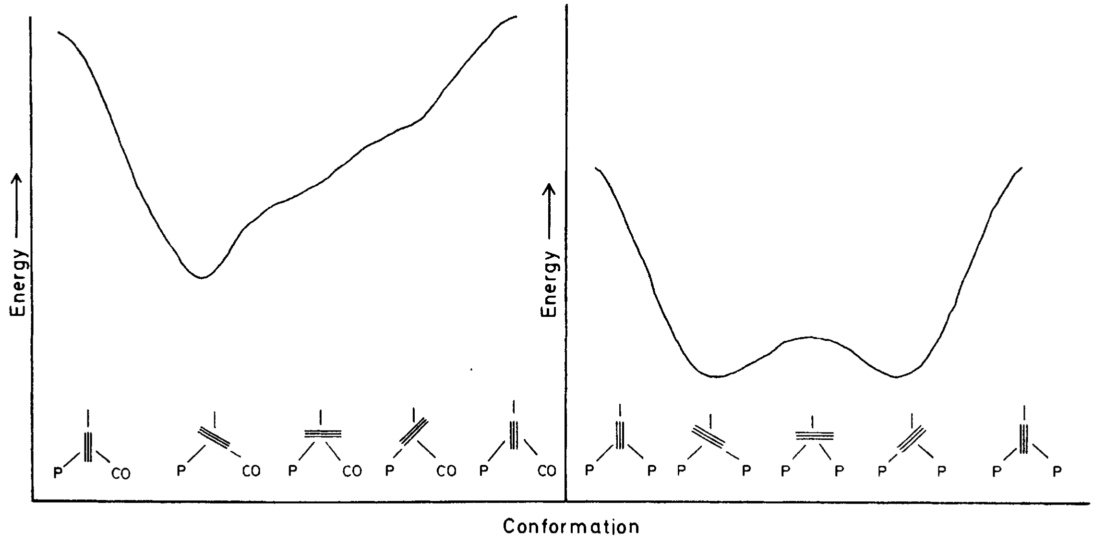

SCHEME 2

EXPERIMENTAL

The instrumentation used and techniques employed were as previously described in ref. 1. Carbon-13 chemical shifts in p.p.m. are relative to $SiMe_4$, positive values to high frequency.

Preparation of (3), *Acetonitrilebis(but-2-yne)(η-cyclopentadienyl)molybdenum Tetrafluoroborate*.—A solution of bis(but-2-yne)carbonyl(η-cyclopentadienyl)molybdenum tetrafluoroborate (2.0 g, 5.2 mmol) and but-2-yne (1 cm^3) in acetonitrile (40 cm^3) was refluxed for 24 h after which time the terminal carbonyl absorption at 2 040 cm^{-1} in the i.r. spectrum had disappeared. The solution was cooled to room temperature and the solvent removed *in vacuo* to afford a yellow powder. This was extracted with methylene chloride (30 cm^3) and filtered off. Addition of diethyl ether and cooling to 0 °C gave large yellow *crystals* of (3) (2.0 g, 95%).

A similar procedure was followed in the preparation of (4), (5), (6), and (7).

Preparation of (8), *Bis(but-2-yne)(η-cyclopentadienyl)(2,2-dimethylpropionitrile)molybdenum Tetrafluoroborate*.—Acetonitrilebis(but-2-yne)(η-cyclopentadienyl)molybdenum tetrafluoroborate (0.5 g, 1.26 mmol) was dissolved in 2,2-dimethylpropionitrile (10 cm^3) and the resulting yellow solution refluxed for 10 min. The solvent was removed *in vacuo*, and the residue extracted with methylene chloride (10 cm^3) and filtered off. Careful addition of diethyl ether (40 cm^3) afforded yellow *crystals* of (8) (0.5 g, 90%).

Preparation of (9), *But-2-ynecarbonyl(η-cyclopentadienyl)(triethylphosphine)molybdenum Tetrafluoroborate*.—An excess of triethylphosphine (0.59 g, 5 mmol) was added to a stirred solution of bis(but-2-yne)carbonyl(η-cyclopentadienyl)molybdenum tetrafluoroborate (1.0 g, 2.55 mmol) in methylene chloride (15 cm^3). After 2 min at room temperature the resultant solution was filtered, and diethyl ether (15 cm^3) added giving purple *crystals* of (9) (0.93 g, 87%).

The complexes (10)—(20), (29), (30), and (31) were prepared in a similar manner.

Preparation of (21), *But-2-yne(η-cyclopentadienyl)bis(triethylphosphine)molybdenum Tetrafluoroborate*.—To a stirred (room temperature) solution of (3) (0.5 g, 1.26 mmol) in methylene chloride (15 cm^3) was added an excess of triethylphosphine (0.59 cm^3, 0.47 g, 4 mmol). The colour of the solution immediately changed to an emerald green, which after 2 h had deepened to a royal blue. Removal of the solvent *in vacuo* left a bright blue powder which was extracted with methylene chloride (10 cm^3) and filtered off. Addition of diethyl ether (40 cm^3) and cooling at 0 °C afforded royal blue *crystals* of (21) (0.6 g, 95%).

Preparation of (22), *But-2-yne(η-cyclopentadienyl)bis(trimethylphosphine)molybdenum Tetrafluoroborate*.—A solution of (3) (0.5 g, 1.26 mmol) in methylene chloride (15 cm^3) contained in a Schlenk tube was cooled to −196 °C and at the same time evacuated. An excess of trimethylphosphine (5 mmol) was distilled into the Schlenk tube by direct pyrolysis of $[AgI(PMe_3)]$ (1.56 g, 5 mmol) at 200 °C. Upon completion of the pyrolysis the Schlenk tube was allowed to warm up. As soon as the solid methylene chloride had melted stirring of the resultant solution was commenced, the colour of the reaction mixture changing from yellow to deep blue. The solvent and excess of phosphine were removed *in vacuo* after the reaction mixture had been stirred at room temperature for 1 h. The resultant blue powder was extracted with methylene chloride (15 cm^3) and filtered off. Addition of diethyl ether (40 cm^3) and cooling (0 °C) gave blue *crystals* of (22) (0.42 g, 74%).

The same general procedure was followed for the complexes (23)—(25) (5 days), (26) (4 days), (27) (1.5 h), and (28) (2 days) except that the noted reaction times at room temperature were required in order for the reaction to go to completion as determined by ^{1}H n.m.r. spectroscopy.

X-Ray Data Collection and Structure Determinations.—*Crystal data.* (12) $C_{20}H_{28}BF_4MoOP$, $M = 498.2$, Monoclinic, $a = 9.158(2)$, $b = 14.726(2)$, $c = 16.581(3)$ Å, $\beta = 94.12(2)°$, $U = 2\,230$ Å^3, $Z = 4$, $D_c = 1.484$ g cm^{-3}, $F(000) = 1\,015.8$, space group $P2_1/c$, Mo-K_α radiation, $\lambda = 0.710\,69$ Å, μ(Mo-K_α) = 6.2 cm^{-1}.

(24) $C_{19}H_{31}BF_4MoP_2$, $M = 504.1$, Monoclinic, $a = 8.661(2)$, $b = 10.293(2)$, $c = 13.580(2)$ Å, $\beta = 106.42(2)°$, $U = 1\,161$ Å^3, $Z = 2$, $D_c = 1.442$ g cm^{-3}, $F(000) = 515.9$, space group $P2_1$, Mo-K_α radiation, μ(Mo-K_α) = 6.5 cm^{-1}.

Measurements. For (12) the crystal was mounted in air, whereas for (24) the specimen required the protection of a Lindemann glass capillary. The unit-cell dimensions and the intensities of all independent reflections with $3 < \theta$-(Mo-K_α) $< 30°$ (12) or $< 26°$ (24) were measured using an Enraf–Nonius CAD-4F diffractometer. The intensities were estimated from continuous θ—2θ scans of 0.60° (12) or 0.70° (24) in θ, increased by 25% at each extremity to allow for background. Counting continued for 90 s or until $\sigma(I)/I < 0.02$, whichever took less time. During each experiment no significant changes were observed in crystal orientation or in the intensities of periodically remeasured check reflections. The integrated intensities and their standard deviations were derived as described previously ($q = 0.04$) [23] and corrected for Lorentz and polarisation effects. The analyses were carried out using the 4 329 reflections for (12) and 2 052 for (24) with $I > 3\sigma(I)$.

Structure analysis. The non-hydrogen atoms in both structures were located by Patterson and Fourier methods and the final values of their co-ordinates and anisotropic temperature factors were obtained by full-matrix least-squares minimisation of $\Sigma w(|F_o| - |F_c|)^2$. In the case of (24) the systematically absent reflections are consistent with the space groups $P2_1/m$ and $P2_1$ although only the latter permits an ordered structure. An ordered model in $P2_1$ finally led to a much more satisfactory refinement than a disordered model in $P2_1/m$. The initial stages of the analysis were, however, hampered by pseudo-symmetry since the (indenyl)MoP$_2$ unit is nearly mirror-symmetrical about the plane $y = \frac{1}{4}$. For both structures the final weighting analyses and difference syntheses ($|\Delta_C| < 0.8$ e Å^{-3}) were satisfactory. Final agreement indices were R 0.041, R' 0.045 for (12) and R 0.039, R' 0.048 for (24). The final atomic vibrational parameters, observed and calculated structure factors, and torsion angles are presented in Supplementary Publication No. SUP 22967 (43 pp.).* In the later stages of each analysis the structure factors included hydrogen contributions [except for the methyl hydrogen atoms in (24)], the hydrogen-atom positions being deduced from those of the adjacent non-hydrogen atoms. For (24) enantiomeric models were considered at a late stage in the refinement and the final calculations refer to the model which gave better structure factor agreement (R 0.040 compared with 0.041).

Various local programs, G. M. Sheldrick's SHELX '78, and C. K. Johnson's ORTEP were used to perform the calculations on an ICL2976 computer. Scattering factors and the anomalous scattering contributions of Mo and P atoms were taken from ref. 24.

We thank the S.R.C. for support.

[0/1135 *Received, 18th July*, 1980]

---

* For details see Notices to Authors No. 7, *J. Chem. Soc., Dalton Trans.*, 1979, Index issue.

REFERENCES

[1] Part 23, P. Caddy, M. Green, J. A. K. Howard, J. M. Squire, and N. I. White, *J. Chem. Soc., Dalton Trans.*, 1981, 400.

[2] R. R. Schrock and P. R. Sharp, *J. Am. Chem. Soc.*, 1978, **100**, 2389.

[3] P. Friedrich, G. Best, E. O. Fischer, and E. O. Huttner, *J. Organomet. Chem.*, 1977, **139**, C68.

[4] B. E. R. Schilling, R. Hoffmann, and D. L. Lichtenberger, *J. Am. Chem. Soc.*, 1979, **101**, 585; and refs. therein.

[5] S. J. McLain, C. D. Wood, and R. R. Schrock, *J. Am. Chem. Soc.*, 1979, **101**, 4558.

[6] (*a*) J. A. Segal, M. L. H. Green, J. C. Doran, and K. Prout, *J. Chem. Soc., Chem. Commun.*, 1976, 766; M. L. H. Green, J. Knight, and J. A. Segal, *J. Chem. Soc., Dalton Trans.*, 1977, 2189; (*b*) M. Bottrill and M. Green, *ibid.*, 1977, 2365; (*c*) M. Herberhold, H. Alt, and C. G. Kreiter, *J. Organomet. Chem.*, 1972, **42**, 413; (*d*) H. G. Alt, *ibid.*, 1977, **127**, 349.

[7] B. E. R. Schilling, R. Hoffmann, and J. W. Faller, *J. Am. Chem. Soc.*, 1979, **101**, 592.

[8] B. C. Ward and J. L. Templeton, *J. Am. Chem. Soc.*, 1980, **102**, 1532.

[9] L. Ricard, R. Weiss W. E. Newton, G. J. J. Chen, and J. W. McDonald, *J. Am. Chem. Soc.*, 1978, **100**, 1318.

[10] W. Beck and K. Schloter, *Z. Naturforsch., Teil B*, 1978, **33**, 1214.

[11] P. L. Watson and R. G. Bergmann, *J. Am. Chem. Soc.*, 1979, **101**, 2055.

[12] J. W. Faller and H. H. Murray, *J. Organomet. Chem.*, 1979, **172**, 171.

[13] P. C. Ford and R. E. Clarke, *Chem. Commun.*, 1968, 1109.

[14] J. L. Davidson, M. Green, F. G. A. Stone, and A. J. Welch, *J. Chem. Soc., Dalton Trans.*, 1976, 738.

[15] J. L. Davidson, M. Green, J. Z. Nyathi, F. G. A. Stone, and A. J. Welch, *J. Chem. Soc., Dalton Trans.*, 1977, 2247.

[16] C. J. Coleman, P. J. McElligott, and D. L. Reger, *J. Organomet. Chem.*, 1979, **171**, 73.

[17] M. H. Chisholm, H. C. Clark, L. E. Manzer, and J. B. Strothers, *J. Am. Chem. Soc.*, 1972, **94**, 5087.

[18] N. M. Boag, Ph.D. Thesis, Bristol, 1979.

[19] H. G. Alt, *J. Organomet. Chem.*, 1977, **127**, 349.

[20] J. W. McDonald, J. L. Corbin, and W. E. Newton, *J. Am. Chem. Soc.*, 1975, **97**, 1970.

[21] H. S. Gutowsky and C. H. Holm, *J. Chem. Phys.*, 1956, **25**, 1228.

[22] A. Allerhand, H. S. Gutowsky, J. Jones, and R. A. Meinzer, *J. Am. Chem. Soc.*, 1966, **88**, 3185.

[23] Lj. Manojlović-Muir and K. W. Muir, *J. Chem. Soc., Dalton Trans.*, 1974, 2427.

[24] 'International Tables for *X*-Ray Crystallography,' Kynoch Press, Birmingham, 1974, vol. 4, pp. 99 and 149.